Reproductive Biology and Endocrinology

BioMed Central

Research

Open Access

The antiestrogen ICI 182,780 induces early effects on the adult male mouse reproductive tract and long-term decreased fertility without testicular atrophy

Hyun Wook Cho[1,2], Rong Nie[1], Kay Carnes[1], Qing Zhou[1], Noaman AQ Sharief[1] and Rex A Hess*[1]

Address: [1]Reproductive Biology & Toxiology, Veterinary Biosciences, University of Illinois, 2001 S. Lincoln, Urbana, IL 61802, USA and [2]Department of Biology, Sunchon National University, Sunchon, 540-742, South Korea, USA

Email: Hyun Wook Cho - hwcho@sunchon.ac.kr; Rong Nie - rongnie97@yahoo.com; Kay Carnes - kcarnes@uiuc.edu; Qing Zhou - qingzhou@wsu.edu; Noaman AQ Sharief - Nomy@NomySharief.com; Rex A Hess* - rexhess@uiuc.edu

* Corresponding author

Published: 18 August 2003

Reproductive Biology and Endocrinology 2003, **1**:57

Received: 03 July 2003
Accepted: 18 August 2003

This article is available from: http://www.RBEj.com/content/1/1/57

Abstract

Background: Estrogen receptors (ER) have important physiological roles in both the female and male reproductive systems. Previous studies using the estrogen receptor-α knockout mouse (αERKO) or antiestrogen treatment in adult rodents have shown that ERα is essential for normal function of the male reproductive tract. In the present study, time-response effects of the antiestrogen ICI 182,780 were determined to better understand ERα function in the adult male.

Methods: Adult male mice, 30 days old, were injected subcutaneously with ICI 182,780 (5 mg) once per week for 17 weeks. Tissues were fixed by vascular perfusion to study the time responses from day 2 to 125 post treatment.

Results: No difference was seen in body weight due to treatment. Testis weight was decreased 18% on day 59 and 21.4% on day 125. Other significant treatment-related effects included the following: 1) dilation of rete testis and efferent ductule lumen; 2) decreased height of the rete testis and efferent ductule epithelium; 3) decreased height of the supranuclear epithelial cytoplasm in efferent ductules; 4) decreased height of the efferent ductule epithelial microvilli, particularly in the proximal ductules; 5) decrease in the PAS-positive granules and endocytotic vesicles in nonciliated epithelial cells of efferent ductules; 6) capping and vesiculation of narrow cells in the initial segment of the epididymis; 7) accumulation of PAS-positive granules in apical cells of the caput epididymis; 8) increase in lysosomal granules in clear cells of the corpus and cauda epididymis; 9) limited induction of atrophic seminiferous tubules and abnormal spermatogenesis; and 10) decreases in the concentration of cauda sperm, progressive sperm motility and decreased fertility.

Conclusions: Antiestrogen treatment of the pubertal male mouse resulted in reproductive effects similar to those observed in the αERKO mouse as early as day 4; however, testis weight did not increase substantially and total atrophy was not observed with extended treatment.

Background

The estrogen receptor (ER)-α knockout mouse (αERKO) was the first animal model to clearly demonstrate the importance of estrogen in male reproductive tract function and fertility [1–10]. The double knockout of ERα and ERβ [10] and the more complete ERα knockout [3] confirmed that ERα is the major receptor responsible for estrogen function in male reproduction.

The major histopathological effect of ERα knockout in the male mouse reproductive tract was centered in the efferent ductules, a small region between the testis and initial segment of the epididymis [4,5,11]. In the αERKO male, there was a failure of efferent ductule epithelium to reabsorb fluid, which caused fluid to accumulate in the rete testis and seminiferous tubule lumen. The long-term consequence of this pathophysiology was backpressure atrophy of the testis, which lead to azoospermia. The important role of estrogen in the male reproductive tract was further demonstrated by transplanting αERKO testicular germ cells into a wild-type recipient mouse testis depleted of germ cells [12,13]. The transplanted αERKO germ cells gave rise to offspring, thus demonstrating that αERKO sperm are capable of fertilizing eggs if the sperm travel through a wild-type reproductive tract environment.

The αERKO mouse continues to be an important animal for the study of estrogen receptor function in the male, but this transgenic animal is a developmental model, as the males lack ERα expression throughout perinatal and postnatal life. Therefore, to test the hypothesis that ERα is necessary in the adult male, and not just for development, the pure antiestrogen ICI 182,780 (AstraZeneca, Macclesfield, Cheshire, UK) was used to block ERs in the pubertal male. In the first study, mice were treated for 35 days and examined for effects. In general, it was concluded that ICI 182,780 treatment replicated most of the effects seen in the αERKO male, except for testicular atrophy and infertility [9].

The rat was also studied for comparison, and although there were similarities to the ICI 182,780 treated mouse, i.e., dilation of rete testis and efferent ductule lumen and decreased height of the ductal epithelium, the time-response approach used in the rat revealed considerable differences between the two species in response to the antiestrogen [14,15]. The rat showed long-term testicular atrophy induced by fluid accumulation and testicular swelling, which led to infertility, similar to the αERKO male. Testicular and efferent ductule effects in the rat were rapid, beginning within 2–4 days after treatment. The rat efferent ductule epithelium also displayed an unusual increase in lysosomal content in the apical cytoplasm of the nonciliated cells, a response not noted after 35 days of treatment in the mouse [9]. Therefore, several questions remained regarding antiestrogen responses in the mouse model: a) Does the mouse require a longer treatment period to show testicular atrophy? b) Is the rat more sensitive to the antiestrogen? c) Would a longer treatment period in the mouse lead to infertility? To answer these and other questions, a time-response study of ICI 182,780 treatment in pubertal male mice was conducted over a 17-week period.

Materials and Methods

Animals and experimental design

This study was conducted in three experiments to fully cover the response period to antiestrogen treatment. The first experiment examined days (d) 8–59 post treatment. Because strong effects were found on d 8, a search for the first response was conducted in an experiment that examined days 1, 2 and 4 post treatment. Infertility was not observed on d 59, therefore, a third experiment was performed to test for effects on days 100 and 125 post treatment.

Adult male C57BL/10 mice at 30 days of age were maintained under constant lighting (12 h light:12 h dark) and temperature (22°C). The University of Illinois Institutional Animal Care and Use Committee approved all experimental protocols. Food and water were available ad libitum for the experimental period. Animals were randomly divided into control (N = 3–6) and treated (N = 3–6) and injected subcutaneously with 0.1 ml of castor oil (controls) or 5 mg of ICI 182,780 (AstraZeneca, Macclesfield, UK) in 0.1 ml, each week for up to 125 days.

Tissue processing

Control and ICI-treated mice were euthanized at specified time points out to d 125 post treatment. The animals were deeply anesthetized with xylazine/ketamine (87 mg/kg and 15 mg/kg, respectively), weighed, and then fixed by vascular perfusion with 4% glutaraldehyde in 0.1 M cacodylate buffer (pH 7.4) for Histopathology. Bouin's fixative or neutral buffered formalin was perfused for immunohistochemistry. Testes, efferent ductules and the epididymides were removed and stored in the same perfusion solution at 4°C until embedded. For microscopic evaluation, tissues were weighed and then washed in cacodylate buffer, dehydrated in an ascending series of ethanol and embedded in glycol methacrylate (Hess et al, 2000). Tissue blocks were cut at 2.5 μm thickness, dried at 35°C, stained with periodic acid-Schiff reaction (PAS), counterstained with Mayer's hematoxylin and mounted for observation. Cauda epididymal sections were also stained with Coomassie blue G250, which highlights the sperm acrosome blue and the nucleus pink.

Immunohistochemistry

Immunohistochemistry was performed only on the efferent ductule tissues, because of its previously determined significance in the αERKO male [4,5,7]. Staining followed previously reported methods of antigen retrieval and indirect secondary antibody labeling [7,16]. Antibodies included, rabbit anti-human carbonic anhydrase-II (CA-II; Chemicon International. Temecula, CA) diluted 1:1000; rabbit anti-rat sodium/hydrogen exchanger-3 (NHE3;Chemicon International. Temecula, CA) diluted 1:1000; rabbit anti-rat aquaporin-1 (AQP1) diluted 1:1000; anti-human ERα (NCL-ER-6F11; Novocastra, Newcastle upon Tyne, UK) diluted 1:1000; sheep anti-human ERβ. [S-40, [17]]; and rabbit anti-rat AR diluted 1:500 [PG21, [18,19]]. Antibody binding was visualized using the avidin-biotin complex (ABC Kit, Vector Laboratories, Burlingame, CA) and diaminobenzidine (DAB). Hematoxylin was applied as a counter stain (Sigma, St. Louis, MO). Sections incubated without the primary antibody but with PBS were used as negative controls for color development on the same slide. Images were captured with a Spot II digital camera (Diagnostic Instruments, St. Sterling Heights, MI) and compiled using Adobe® Photoshop® (Adobe Systems, San Jose, CA).

Sperm Concentration and Motility

To determine sperm concentration in the cauda epididymis for the first 59 days of the study, paraffin histological sections of the distal cauda epididymis were sectioned at 20 μm thickness and stained with hematoxylin and eosin. The slides were viewed using a video camera mounted on an Olympus microscope with a plan-apochromatic 100X objective. Observed fields were selected by a systematic, uniform random sampling method, using the Stereo Investigator software, v3.0 (MicroBrightField Inc., Colchester, VT) and a motorized stage. Sperm heads were counted in a counting frame having a total of 20,000 μm^3 per tubule. Ten replications per epididymis were made.

On day 125 post treatment, sperm concentrations were determined using minced cauda epididymides and a dual-sided semen analyzer system (Hamilton Thorne Research, Beverly MA). The cauda epididymis on one side of the 125 day mouse was dissected prior to perfusion and was placed in a sterile Petri dish containing 1 ml of modified Hank's Balanced Salt Solution (m-HBSS) for sperm motility analysis. The cauda was minced and incubated for 5 minutes at 37°C to allow sperm to swim into the media. At the end of the incubation time, a 100 μl sample of the media containing the sperm was diluted with 900 μl of the m-HBSS solution for sperm analysis. Each sperm analysis chamber was loaded with 14 μl of the diluted sperm by capillary action. Analysis chambers were immediately placed into the specimen holder of TOX-IVOS computer assisted sperm analysis system that had been calibrated for mouse sperm samples. The samples, chambers and specimen holder were maintained at 37°C throughout the entire measurement period. Six fields were analyzed from each of the two chambers and the results averaged.

Image analysis

Tissues were photographed using a Spot-II digital camera mounted on an Olympus Microscope and Plan-apochromatic lenses (Olympus America Inc, NY) and saved in Adobe Photoshop (Adobe Systems, Inc., San Jose, CA). Morphometry data from days 8, 16, 59 and 125 post treatment are included. The digital images from both reproductive tracts of 3 control and 3 ICI-treated animals on each post treatment day were analyzed by Scion Image Software (Scion Corporation, Frederick, MD). Luminal diameter of 10 seminiferous tubules (stages VII-VIII) was determined per mouse per testis, by measuring the widest diameter in cross-section. However, for day 125 all sem-

Table 1: Effects of ICI 182,780 on body and testis weight.[a]

Day of treatment	Body Weight (g)		Testis Weight (mg)	
	Control	ICI-Treated	Control	ICI-Treated
8	17.99 ± 2.22	19.8 ± 1.17	71.4 ± 1.81	83.2 ± 5.87
10	16.48 ± 0.81	22.66 ± 0.42	68.0 ± 2.96	78.9 ± 4.33
12	19.74 ± 1.58	24.41 ± 1.43	85.1 ± 2.49	90.9 ± 0.86
14	22.17 ± 0.98	21.57 ± 0.15	91.0 ± 3.40	91.0 ± 2.93
16	22.65 ± 0.46	24.3 ± 0.15	84.9 ± 1.40	96.3 ± 1.70[b]
25	25.67 ± 0.66	26.11 ± 0.56	96.5 ± 2.59	94.6 ± 2.85
59	26.63 ± 0.44	30.19 ± 1.27	128.7 ± 5.37	105.0 ± 7.03[b]
125	29.97 ± 0.45	31.97 ± 0.78	95.2 ± 2.58	74.8 ± 4.75[b]

[a] Values are mean ± SEM [b] $p < 0.05$.

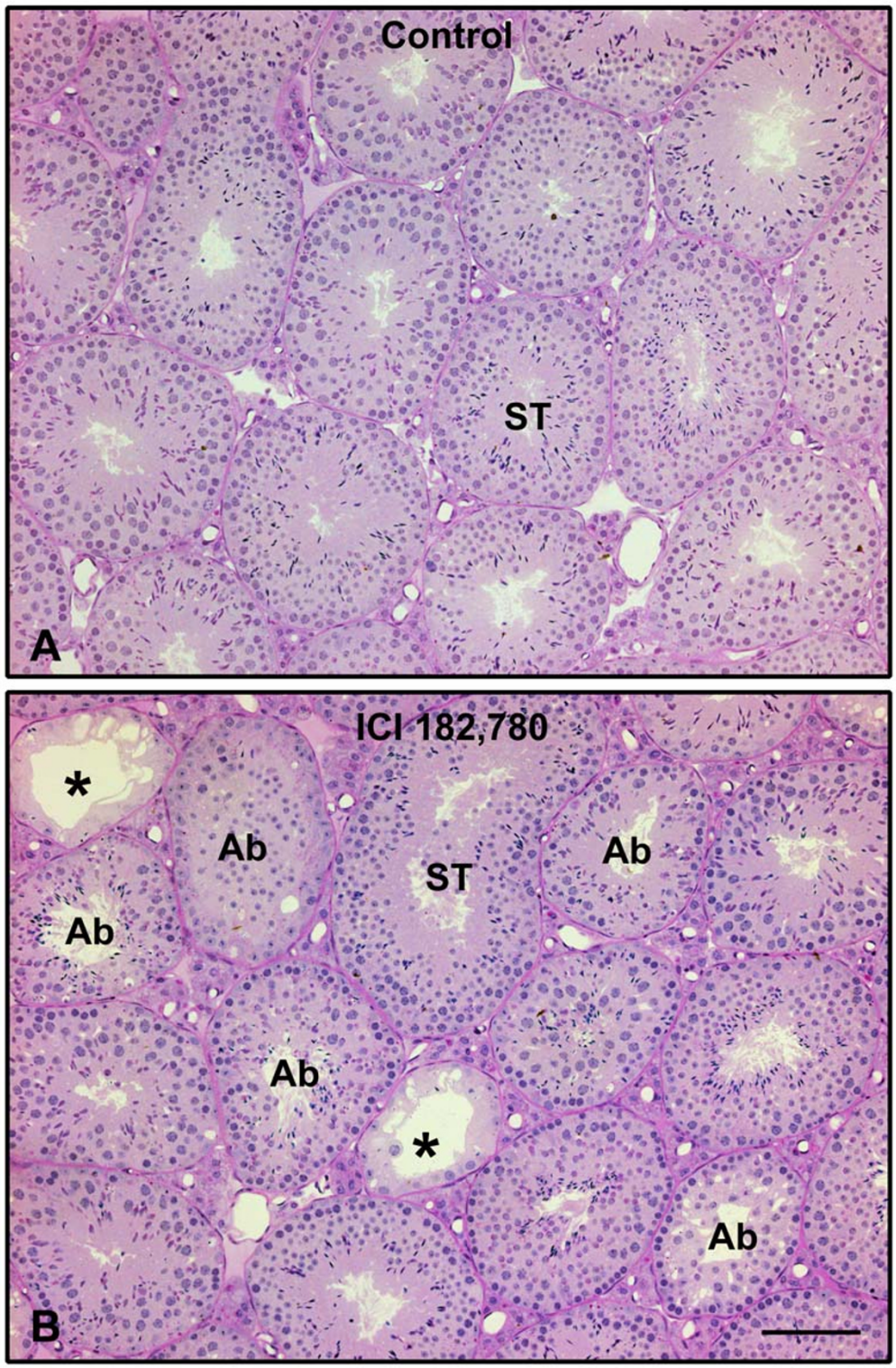

Figure 1
Testis sections on day 125 from control (A) and ICI 182,780 treated mice (B). Control testis shows normal spermatogenesis with seminiferous tubules (ST) filled with germ cells. In the treated testis, several tubules (ST) show normal spermatogenesis, but other show abnormal spermatogenesis (Ab) and two tubules are atrophic (*). The abnormal tubules show decreases in spermatids, sometimes only in portions of the epithelium. Bar = 100 μm.

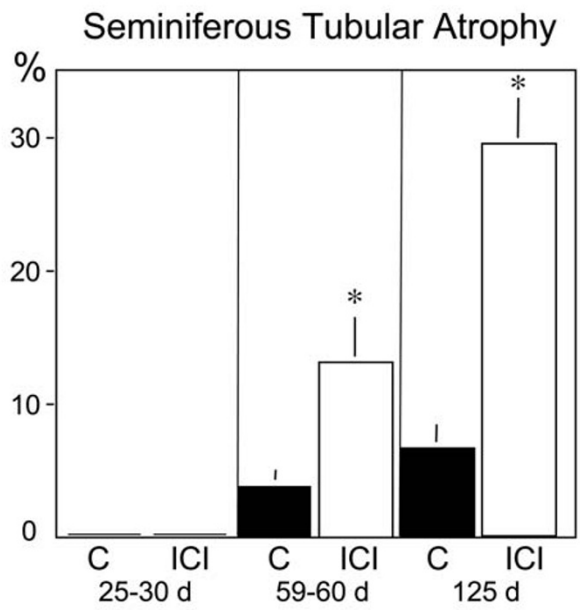

Figure 2
Seminiferous tubular atrophy. Even control testes show limited atrophic tubules with aging of the males, but beginning on day 59 the number of atrophic tubules was significantly (*) increased in the ICI-treated testes. Means ± SEM; ($p < 0.05$).

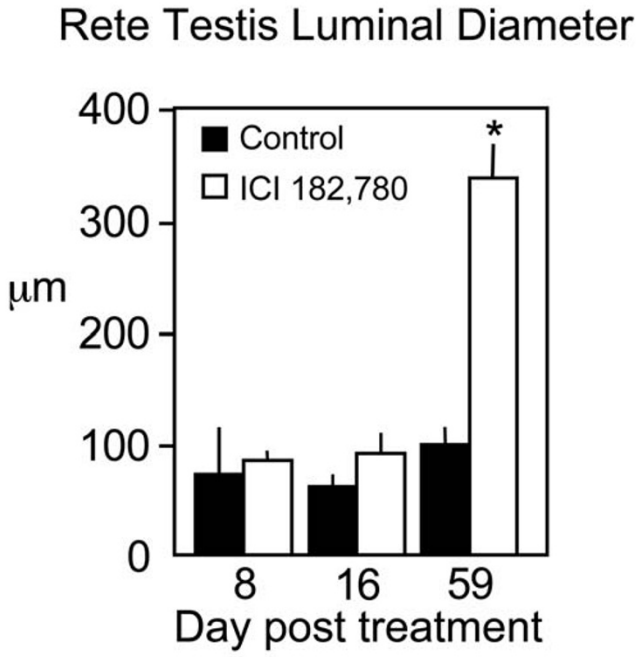

Figure 3
Rete testis luminal diameter. The antiestrogen treatment model induced a highly significant increase in the diameter by day 59 ($p < 0.05$).

iniferous tubules per testis were measured for diameter because some tubules were atrophic and stage of spermatogenesis was not determined. Luminal diameter of the rete testis was determined in 3 testes per treatment group. Luminal diameter of proximal efferent ductules was determined in 5 sections per mouse. Cell height was measured from the base to the apex in 30 epithelial cells of the rete testis region, or to the microvillus tip in 30 nonciliated cells from non-oblique sections of the proximal efferent ductules per mouse. The supranuclear cytoplasmic height was determined by measurement from the top of the nucleus to the microvillus tip in the nonciliated cells in the proximal efferent ductules.

Fertility

Individual mice of control and ICI-treated groups on day 50, day 93, or day118 after treatment were mated with 3 female mice of the same age and strain for one week, then separated. One week after separation, the females were euthanized by sodium pentobarbital injection and the uterine horns opened. The number of embryos, number of implantation sites and resorptions/stillbirths were counted. If at least one female per mating had live births, the male was considered fertile. Subfertility was indicated by a reduction in the number of live births or an increase in the number of resorptions.

Statistical analysis

Data are presented as means ± SEM. To compare morphological differences between controls and treatment groups, means were analyzed by two-way ANOVA followed by individual paired t-test for each time point ($P < 0.05$). Proportion data were analyzed by the chi-square test with a probability of less than 5% considered significant.

Results

Body and organ weights

There was no significant difference in body weight between control and the treated groups (Table 1). Testis weight was increased on day 16 but decreased on days 59 and 125. The increase in weight on day 16 is likely due to a discrepancy in animal ages at the time of treatment. When this time point was repeated using mice at 30 day of age, the difference disappeared (data not shown).

Testis and rete testis

Spermatogenesis appeared normal until day 59, as which time focal regions showed seminiferous epithelial disruption and the beginning of isolated tubular atrophy. However, normal spermatogenesis was seen in most seminiferous tubules throughout the 125-day treatment

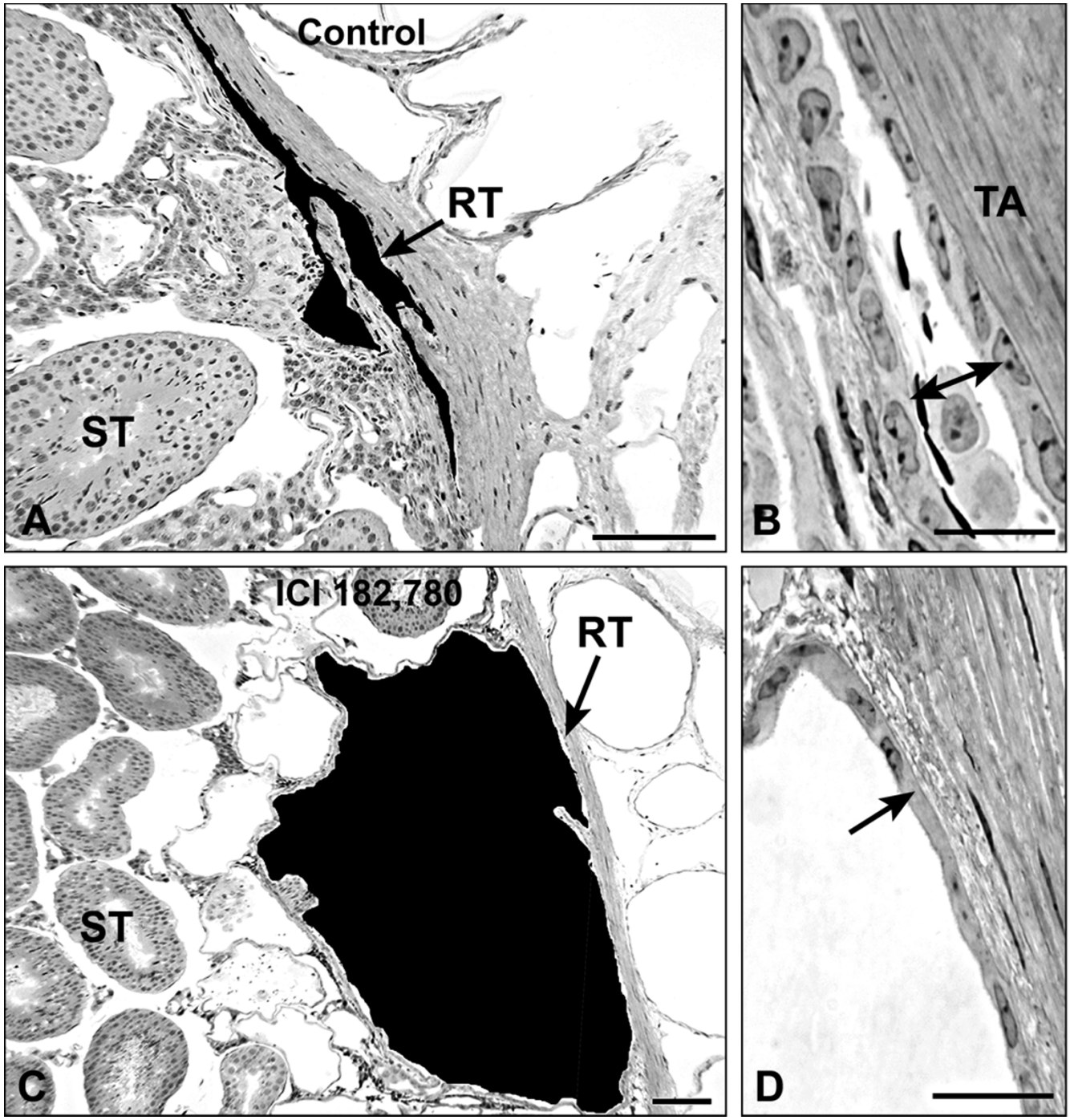

Figure 4
Rete testis histology from control and ICI-treated groups on day 59 post treatment. A. Control rete testis filled in with black shading to show a very thin channel (RT) with seminiferous tubule on the left (ST). B. Higher magnification of control showing a nearly cuboidal epithelium with narrow lumen (double arrow). The side adjacent to the tunica albuginea (TA) was thinner than the side adjacent to the seminiferous tubules. C. ICI 182,780 treated rete testis (RT; filled with black shading) showing strong dilation (double arrow). Seminiferous tubules (ST) are normal. D. ICI treated rete epithelium that is decreased in height (arrow). Bar = 100 μm for A, C. Bar = 25 μm for B, D.

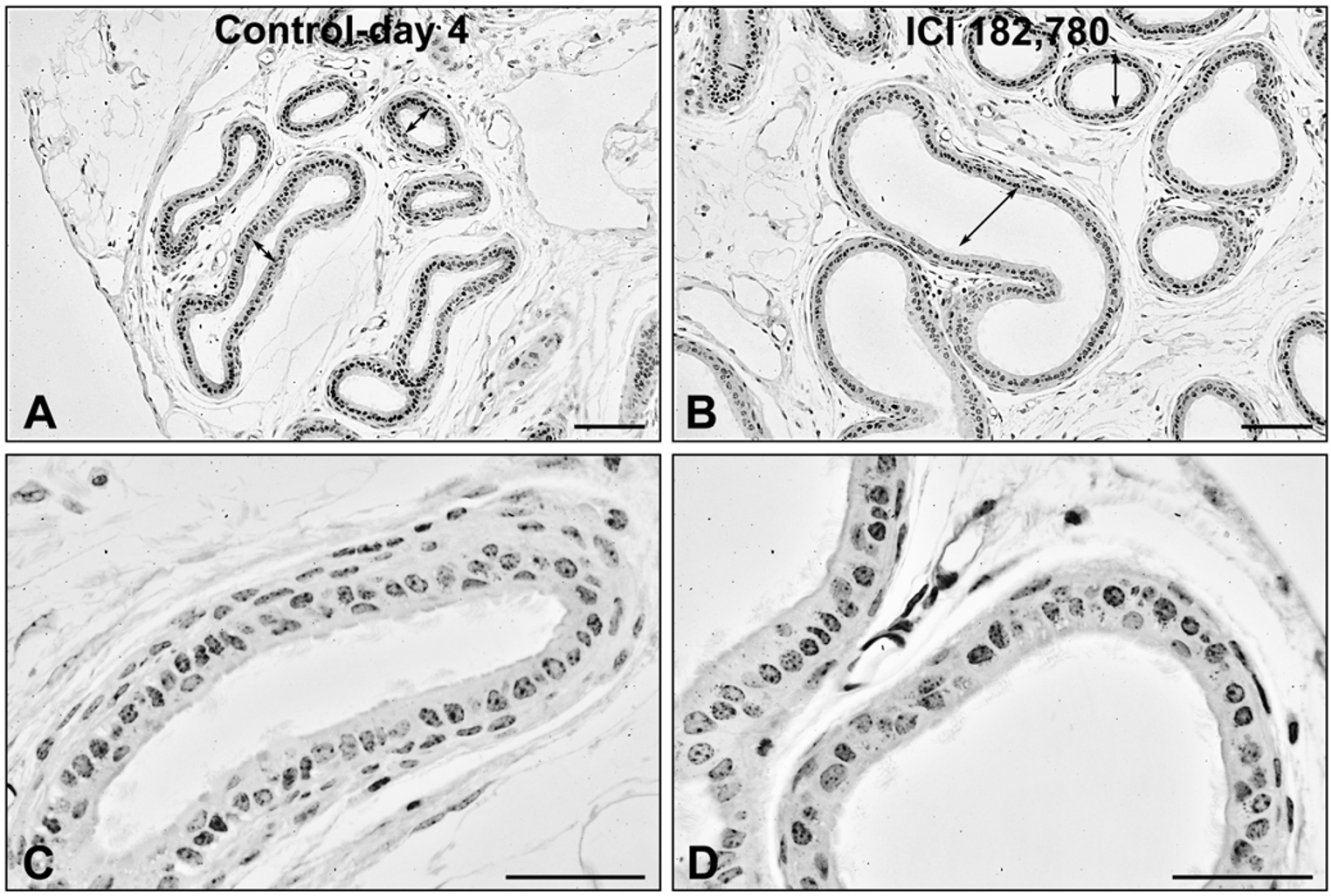

Figure 5
Proximal region of efferent ductules from control (A, C) and ICI-treated (B, D) groups on day 4 post treatment. A. Control efferent ductules have a narrow diameter (double arrows). B. ICI treated ductules are dilated (double arrows) extensively by day 4. C-D. Higher magnification shows no change in the epithelium on day 4 post treatment. Bar = 50 μm for A, B. Bar = 25 μm for C, D.

period (Fig. 1). Seminiferous tubular diameter showed no difference between treatment groups until day 125, when mean tubular diameter in the treated group was 164.8 ± 0.8 μm compared to 187.1 ± 4.0 μm for the controls, a significant difference of 11.9% ($p < 0.01$). This change was due to a significant increase in the number of atrophic seminiferous tubules from day 59 to 125 (Fig. 2). The luminal diameter of rete testis was increased 241% on day 59 in the treated group (Figs. 3 and 4A,4B,4C,4D) and remained dilated throughout the 125-day period. Epithelial cells lining the rete testis were variable in height, but showed significant decreases (22% overall decrease across all time periods) beginning on day 8 and continuing to day 125 (Figs. 4B,4D).

Efferent ductule

As early as day 4 post treatment, ICI 182,780 treatment caused luminal dilation in the proximal efferent ductules (Fig. 5). However, luminal dilation on day 4 was noted without a decrease in epithelial height. Tubule dilation continued throughout the treatment period, reaching a maximum increased dilation of 140% on day 125 (Fig. 6). The conus and common efferent ductules also showed significant dilation at all time points (data not shown). Height of epithelial cells in the efferent ductules was also decreased after treatment on days 8–125 (Fig. 7); however, on day 125 epithelial height was highly variable in the treated males and the mean was approaching that of the controls, although areas were nearly squamous in appearance (Fig. 8).

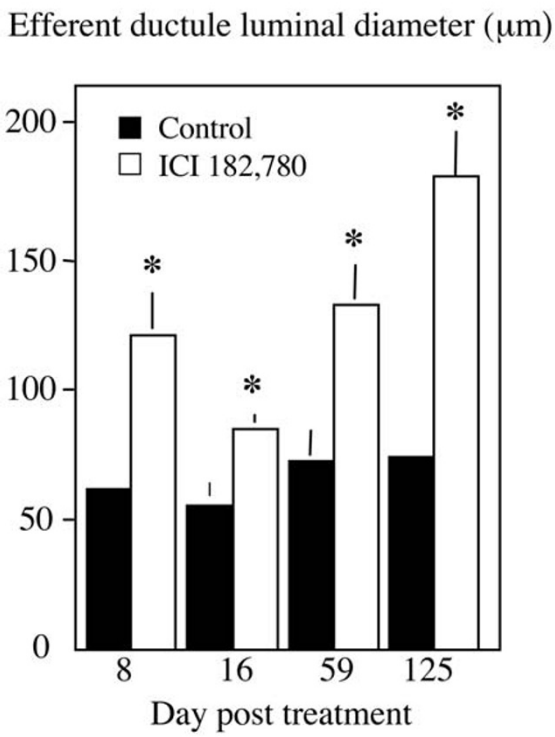

Figure 6
Proximal efferent ductule luminal diameter. The ductule lumen was dilated significantly throughout the treatment period. Means ± SEM. Significant differences (*) between control and treated at each time point are noted ($p < 0.05$).

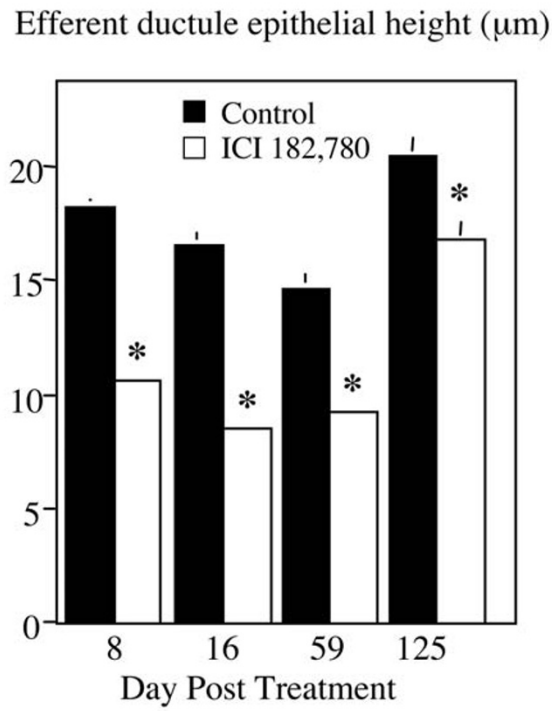

Figure 7
Proximal efferent ductule epithelial cell height. Cell height was reduced significantly at all time points. However, on day 125 post treatment the mean difference was less than previous periods and the height showed greater variation. Means ± SEM ($p < 0.05$).

The supranuclear cytoplasm, the region that contains an abundant endocytotic apparatus in nonciliated cells of the efferent ductule, was consistently reduced by nearly 50% in the treated group, compared to controls (Fig. 9). On day 125, the supranuclear region was increased in both treated and controls, but there still remained a significant reduction in height in some proximal ductule areas (Fig. 8).

PAS positive lysosomal granules were numerous in the supranuclear cytoplasm of control nonciliated cell in the proximal region (Fig. 8A,8C,8E). The conus and common regions in control animals contained fewer lysosomal granules (data not shown). ICI 182,780 treatment caused a reduction in the number of lysosomes and vesicles in all regions, but in some regions the effect was more dramatic (Fig. 8B,8D,8F). The reduction in lysosomes was associated with a decrease in supranuclear cytoplasm (Fig. 9). With decreased height of the epithelium, the nuclear shape was changed from nearly round or slightly columnar (controls) to a more flattened morphology (Fig. 8).

ICI 182,780 treatment also caused microvilli along the luminal border of the nonciliated cell to shorten significantly (Fig. 10). Mean height of microvilli in the treated tissue was decreased by 18% in the proximal efferent ductule epithelium. Microvilli in the conus and common regions were decreased in height by 16% and 6%, respectively (data not shown).

Efferent ductule immunohistochemistry

On day 125 post treatment, the expression of ERα was decreased, while ERβ showed no change in expression in the efferent ductule epithelium (Fig. 11A,11B,11C,11D). NHE3 was completely absent along the apical border of the treated nonciliated cells (Fig. 11E,11F). AQP1 were decreased significantly along the apical border in nonciliated cells of the ICI 182,780 treated efferent ductules, but along the basolateral border all staining was eliminated (Fig. 11G,11H). CAII was also decreased significantly along the apical cytoplasm of the efferent ductule epithelium (Fig. 11I,11J).

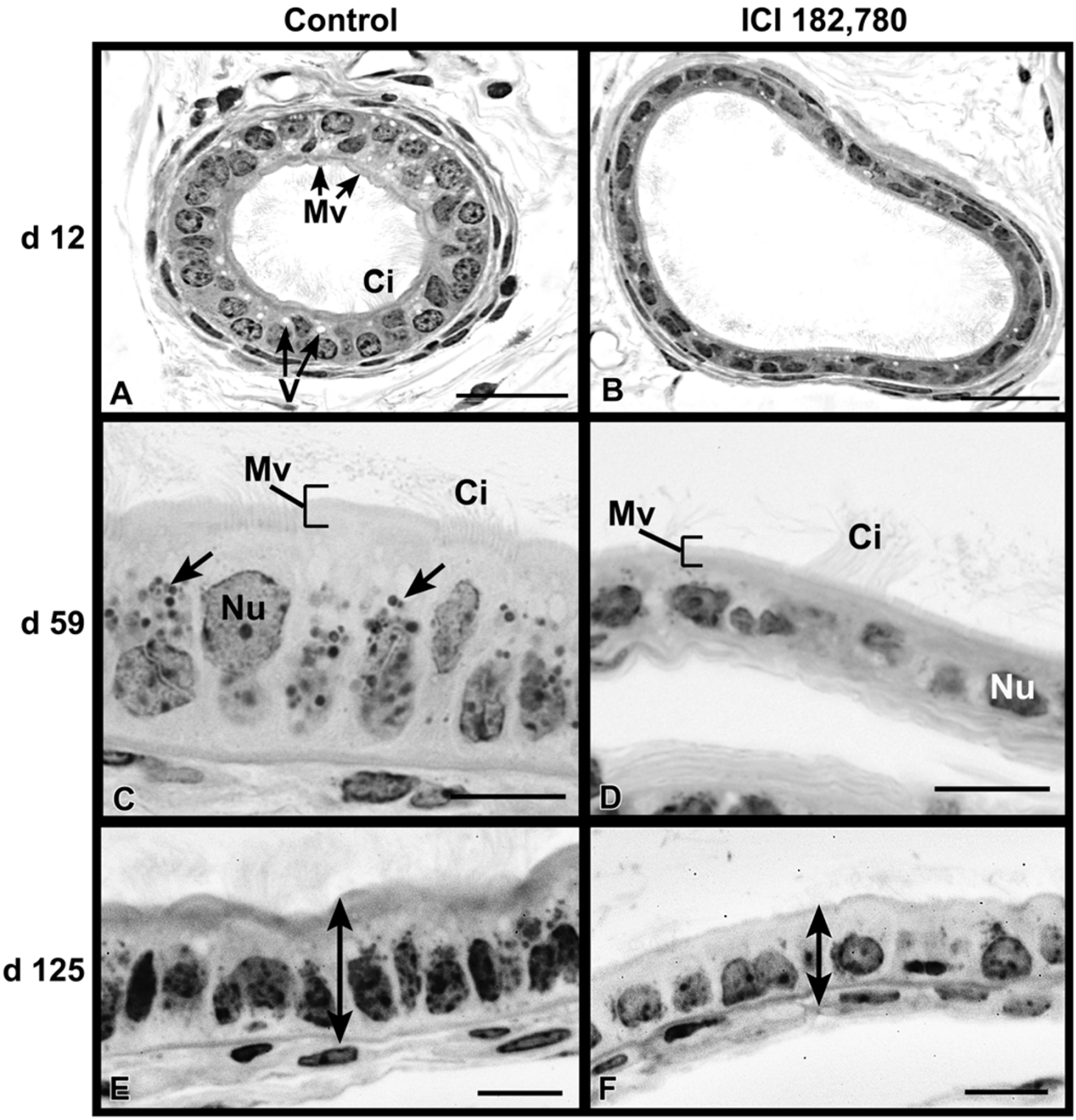

Figure 8
Higher magnification of the proximal efferent ductule epithelium in control (A,C,E) and ICI-treated (B,D,F) males. A, B. Day 12 post treatment showing nearly cuboidal epithelium in control tissue during early puberty but a shortened epithelium in the ICI treated (B). Ci, cilia; Mv, microvilli; V, endocytotic vesicles. C, D. Day 59 post treatment the epithelium has reached it maximum height in control samples (C), however, the height is quite variable between regions. Nuclei (Nu) of ciliated cells are found more apical than the nonciliated cells. Apical cytoplasm of nonciliated cells contained an abundance of PAS-positive granules, previously identified as lysosomes (arrows). Microvilli (Mv) are tall and easily distinguished from the long cilia (Ci). In the ICI-treated ductules, microvilli are short and the nuclei are flattened. E,F. Day 125 post treatment. The control ductule epithelium is columnar (double arrow) and contains numerous PAS-positive granules. In some regions of the ICI-treated group, the epithelium remains severely shortened in height (double arrow). Bar = 50 μm for A, B. Bar = 25 μm for C-F.

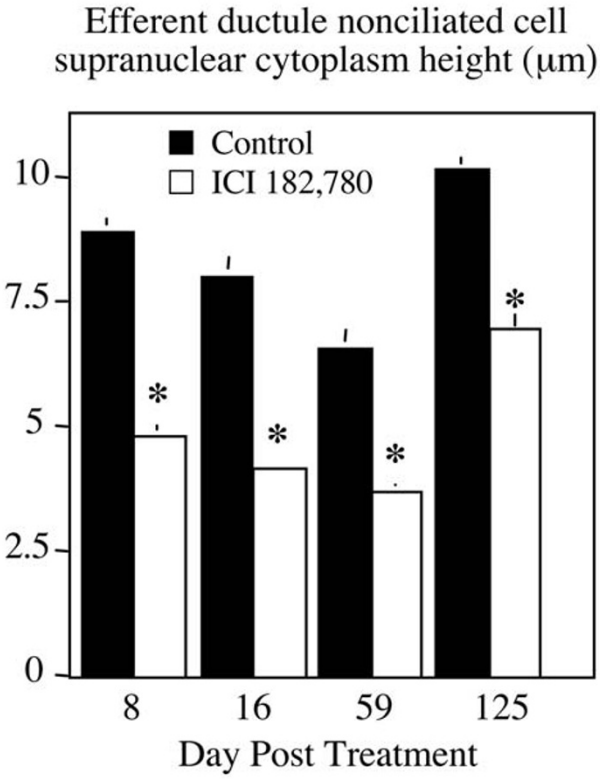

Figure 9
Proximal efferent ductule nonciliated cell supranuclear cytoplasmic height. The data represent means ± SEM. The increase seen on day 125 may be due to this day being a separate experiment, although there may be some increase due to aging. Significant differences (*) between control and ICI-treated means are noted ($p < 0.05$).

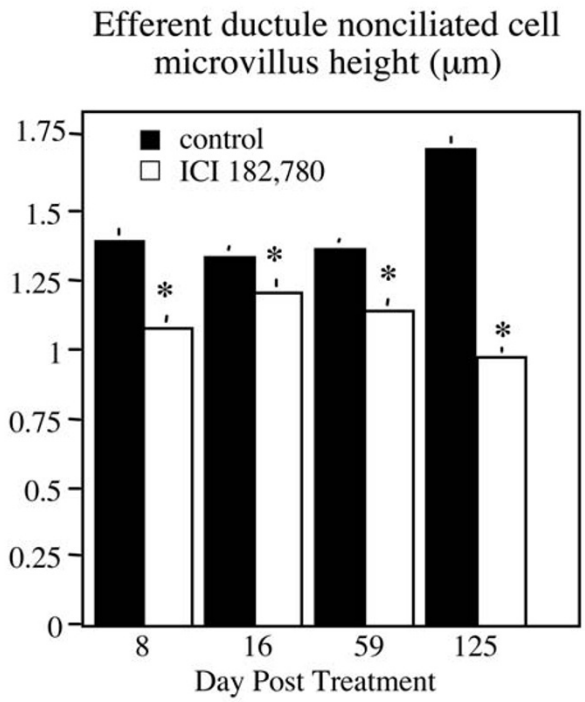

Figure 10
Proximal efferent ductule nonciliated cell microvillus height. The data represent means ± SEM. At all time points there was a significant decrease in height (*) between control and ICI-treated cells ($p < 0.05$).

Epididymis

In the initial segment, narrow cells show slight protrusion of their apical vesiculated cytoplasm into the lumen, while in the ICI 182,780 treated tissues the narrow cell cytoplasm contained more vesicles and protruded further into the lumen (Fig. 12). By day 125 post treatment, apical cells in the caput epididymis were engorged with PAS-positive lysosomal-like granules (Fig. 13), with some granules nearly as large as the nucleus. In the corpus and cauda regions post treatment, the clear cells showed an increase in the number and size of vesicles in both principal and the clear cells (Fig. 14). This observation was present as early as day 8 post treatment. The vesicles were mainly supranuclear in location. Clear cells also contained an increase in the number of PAS positive granules in their basal cytoplasm after treatment (Fig. 14). After antiestrogen treatment, principal cells of the distal cauda also showed an increase in the number and size of cytoplasmic vesicles, as early as day 8, as well as an increase in the number of PAS-positive granules (Fig. 14).

Histological sections of cauda epididymis on day 59 post treatment were also stained with Coomassie blue G250 to highlight the sperm acrosome and nucleus. Several abnormalities were noted in the ICI-treated sections (Fig. 15). In control cauda epididymis, the sperm were aligned nearly parallel and the cytoplasmic droplet was located on the mid-tail region. At higher magnification, the sperm heads were attached to the tail and displayed a prominent staining of the acrosomic region along the dorsal edge of the nucleus (Fig. 15A,15B). In the ICI-treated samples, sperm were less concentrated and appeared disorganized, with few nuclei attached to tails (Fig. 15C). At higher magnification, detached sperm nuclei were misshaped and often appeared to have reduced staining of the acrosome (Fig 15D,15E) and the tails were looped around the cytoplasmic droplets (Fig. 15F).

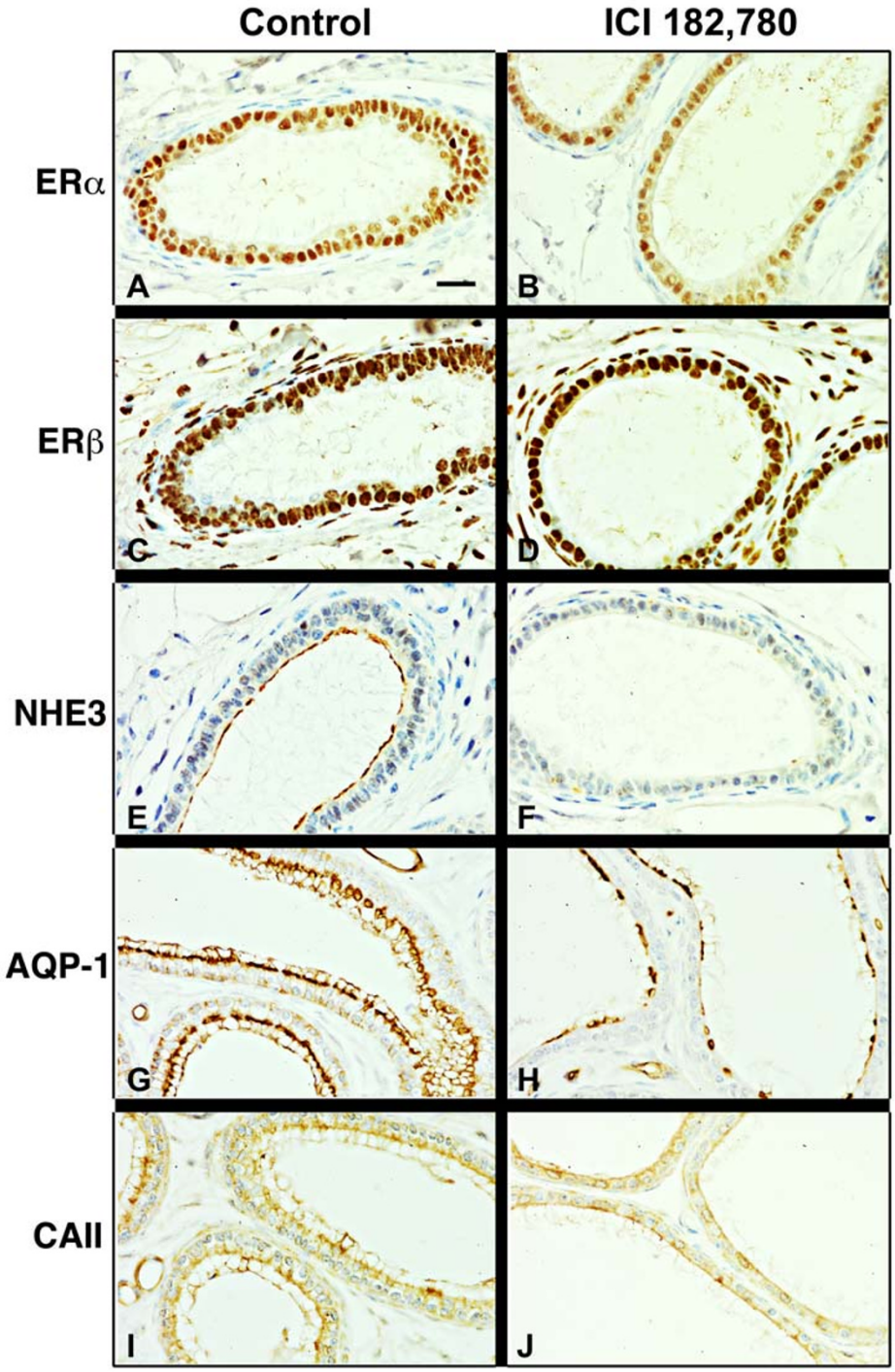

Figure 11
Immunohistochemical staining of proximal efferent ductules on day 125 post treatment. A,B. ERα is expressed abundantly in control efferent ductule epithelium, with slightly less staining in the ciliated cells (apical nuclei), but is reduced in the ICI-treated tissue. C,D. ERβ is also abundant in efferent ductule epithelial cells, both in the controls and treated samples. E,F. Sodium/hydrogen exchanger (NHE3) is stained heavily along the apical border of the nonciliated cells of control tissue, but is absent in the ICI-treated tissue. G,H. Aquaporin-1 (AQP-1) is abundant along the microvillus border of the control ductules, but is diminished in the treated tissue, although intensely stained along the apical border of some cells. I,J. Carbonic anhydrase II (CAII) is present along the microvillus border and in apical cytoplasm of control ductules, but is greatly reduced in the epithelium of treated tissues. Bar = 25 μm.

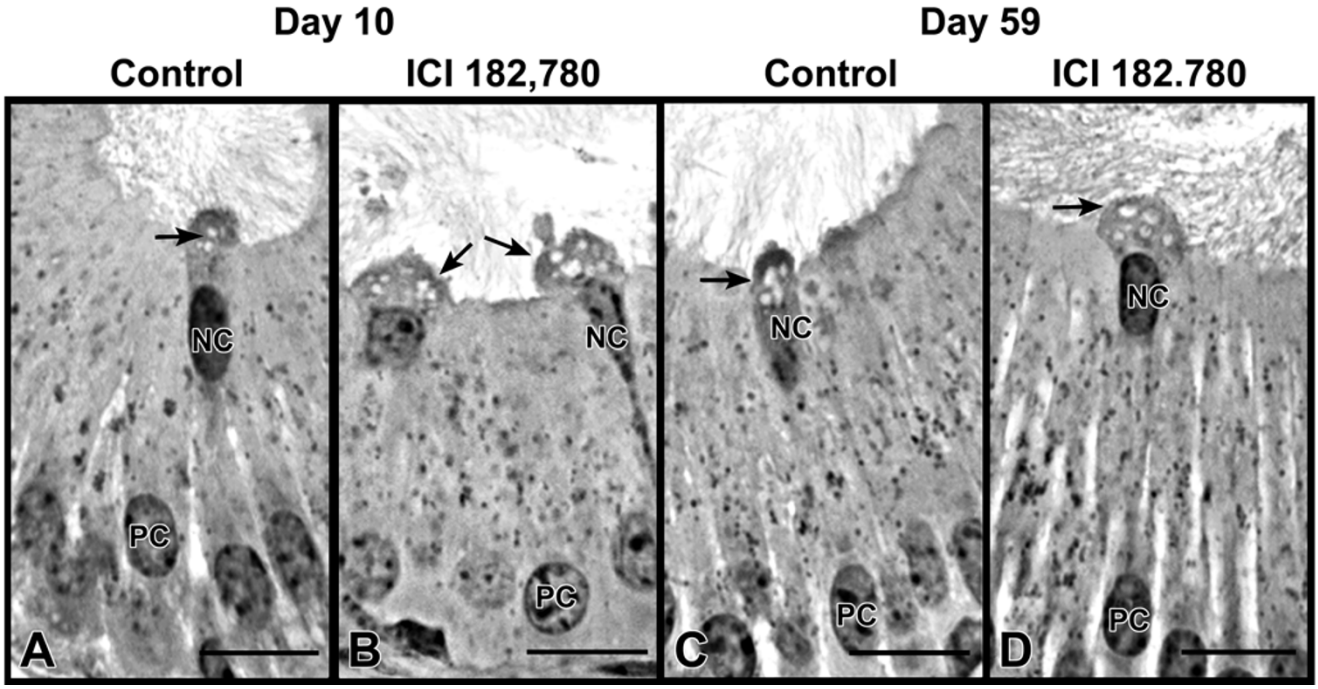

Figure 12
Initial segment of the epididymis on days 10 and 59 post treatment. A. Control section on day 10 showing the narrow cell (NC), whose apical cytoplasm protrudes (arrow) into the lumen. Principal cell (PC) nuclei lie beneath the narrow cell. B. ICI 182,780 treated section on day 10 showing two narrow cells with more extensive apical cytoplasmic vesiculation extending into the lumen (arrows). C. Control day 59 showing normal epithelium with narrow cells having a modest extension into the lumen (arrow). D. ICI-treated day 59 showing a narrow cell extension (arrow) into the lumen, similar to that seen on day 10. Bars = 12.5 μm.

Reproductive performance

There was no difference in fertility, the number of embryos or the number of resorptions and stillbirths per female between the control and treated groups on day 59 and 100 (data not shown). However, cauda sperm concentrations in the treated groups did not show the normal increase associated with increasing age and beginning on day 16 through 125 post treatment there was a significant difference from controls (Fig. 16). On day 125 post treatment, cauda sperm concentration in the ICI-treated males was decreased 40%, sperm motility was decreased 80% and 4 of 6 treated males were infertile (Table 2). The treated males that sired offspring had a lower mean number of births (litter size), but due to large variation in both groups, the means were not significantly different. However, there a significant increase in the incidence of resorptions and stillbirths (Table 2).

Discussion

The present study demonstrates that the mouse ICI 182,780 treatment model, when extended from 4 days to 125 days post treatment, resembles the αERKO model in nearly every feature, except for the transient increase in testis weight and testicular atrophy. The decrease in sperm concentration in cauda epididymis and luminal dilation of the rete testis and efferent ductules following treatment clearly support the overall hypothesis that a functional ERα is required for normal fluid reabsorption in the efferent ductules, as concluded from prior studies of the αERKO male [4,7].

In the present model, treatment was started at 30 days of age. This age represents early puberty and the males were still growing, as evidenced by the increase in body and testis weights in controls and treated animals over the next 60 days. Except for an unexplained difference in testis weight on day 16 post treatment, there was no effect on testis weight out to day 25, similar to a previous short-term study [9]. However, on day 59 of treatment testis weight differences began to appear, with a decrease in the treated animals. Thus, with a longer treatment period the mouse showed limited atrophy of seminiferous tubules, but not total atrophy as seen in the αERKO males [4].

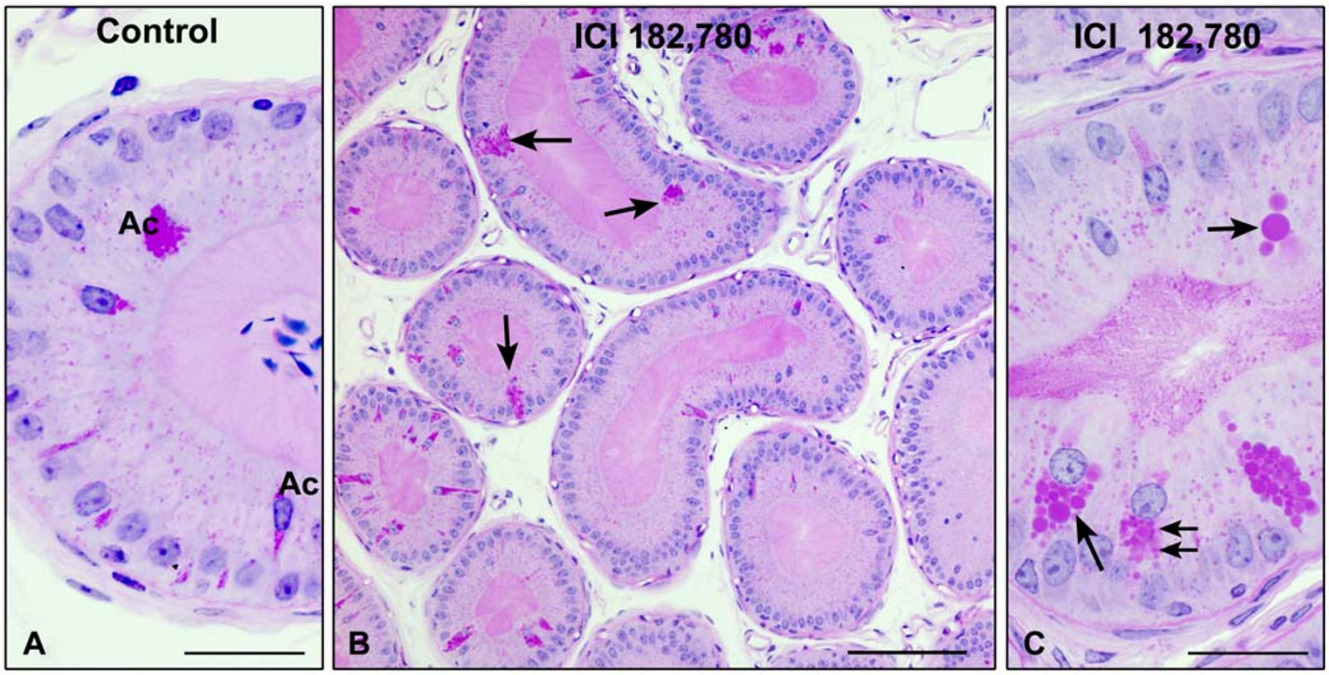

Figure 13
Caput epididymis on day 125 post treatment. A. Control caput showing the apical cell (Ac) with and without apical PAS-positive granules. B. ICI-treated caput region showing increased number of the apical cells (arrows) that are engorged with PAS-positive granules. C. Higher magnification of ICI-treated caput region showing an increased size of the PAS-positive granules (large arrows) and the appearance of granules below the nucleus (small double arrows). Bars = 25 μm for A and C. Bar = 100 μm for B.

At the beginning of puberty, spermatogenesis appears normal in the αERKO testis, but as the male ages seminiferous tubules begin to degenerate [1]. The αERKO testis weight nearly doubles in approximately 40 days, starting at puberty; then testis weight declines and eventually total testicular atrophy occurs at 185 days of age [4]. ICI 182,780 treatment in the rat induces a similar pattern of effect, with both testicular swelling and long-term atrophy of the testis, nearly identical to the αERKO male [14,15]. Why the mouse testis did not respond with a similar increase in testis weight and then atrophy remains a major question. However, the rete testis was dilated in the mouse, as in αERKO and ICI-treated rat males, suggesting that ability of the mouse testis to handle fluid accumulation is dependent upon developmental factors that are lacking in the αERKO male. One possibility is that the mouse epididymis is capable of compensatory reabsorption of the excess fluid. Future studies are required to understand these differences in response.

The effects observed on spermatogenesis did not appear to be due to fluid accumulation because there was no dilation of the seminiferous tubular lumen, in contrast to what was discovered in the αERKO testis [4]. Furthermore, abnormal spermatogenesis did not occur until day 59, suggesting that the degenerative process required long-term inhibition of ER. Because ICI 182,780 blocks both ERα and ERβ [20], the delayed testicular response may be due to ICI's inhibition of ERβ and not ERα. ERα is not expressed in the seminiferous epithelium, but ERβ is abundant in Sertoli and germ cells [16,21–25]. Therefore, ICI's effects on the epithelium may be through long-term inhibition of ERβ. It is interesting that the aromatase knockout mouse also shows a delayed disruption of spermatogenesis [26,27], similar to the effects of ICI 182,780 in the mouse testis. Although the ERβ knockout mouse shows no apparent phenotype [3,10,28], in light of the current findings, it would be worthwhile to examine the βERKO male for specific aging effects on the testis.

Dilation of the rete testis lumen was less extensive following ICI 182,780 treatment, compared to the αERKO mouse [9]. The present study demonstrated that this effect begins sooner than previously thought, with dilation being observed on day 10. On the other hand, the rete

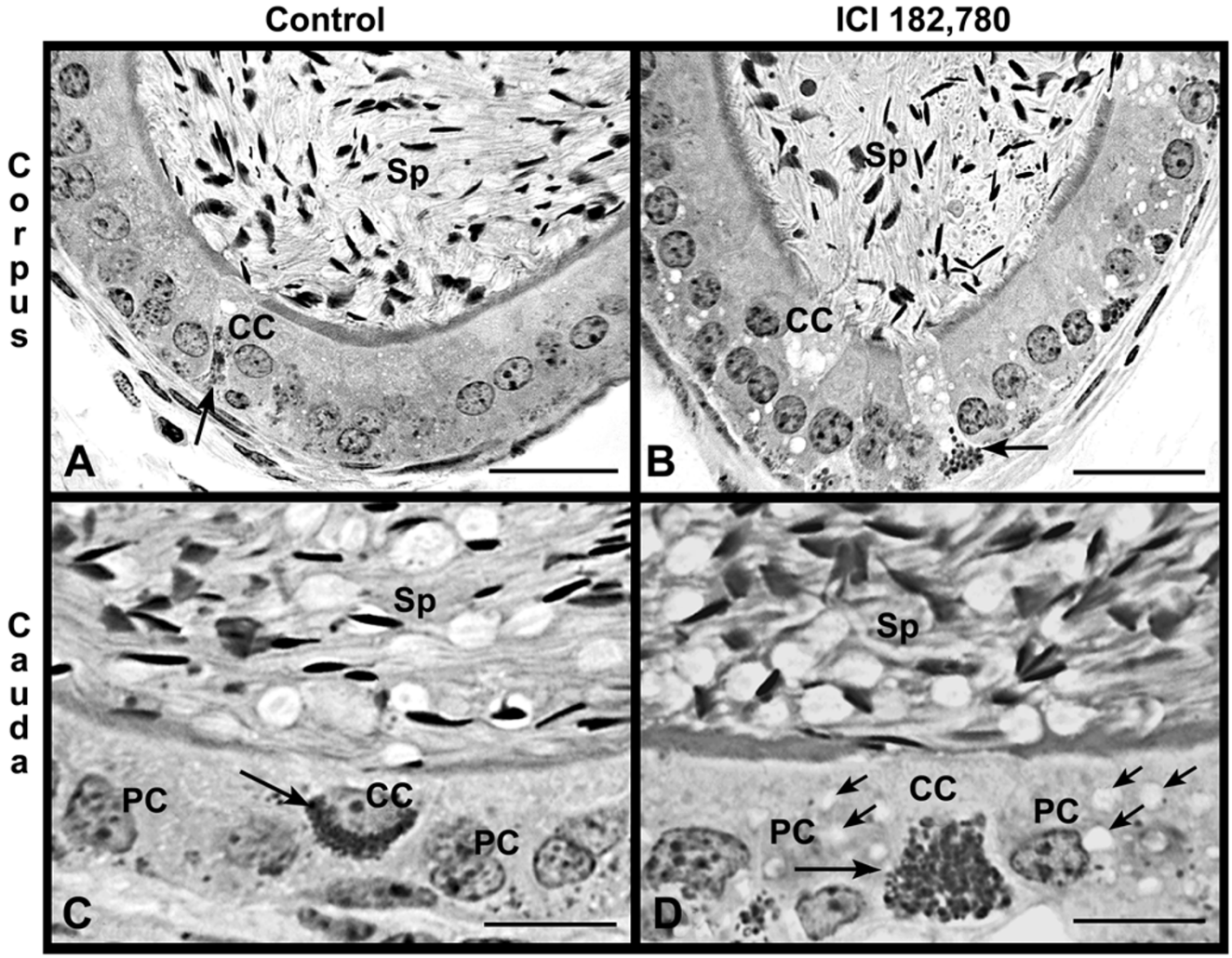

Figure 14
Corpus and cauda regions of the epididymis from control (A,C) and ICI-treated (B,D) males on day 8. A. Corpus epididymis in control. PAS-positive granules (arrow) are distributed in the perinuclear region of a clear cell (CC) that also contains a few apical vacuoles. Sperm (Sp) appear normal in the lumen. B. Corpus epididymis in ICI-treated. The clear cell appears to contain an increased number of apical vesicles and basal granules (arrow). Sperm appear normal in the lumen on day 8. C. Cauda epididymis in control. PAS-positive granules (arrow) are abundant in the perinuclear region of a clear cell. The principal cells (PC) have small vacuoles in the cytoplasm. Sperm (Sp) appear normal in the lumen. D. Cauda epididymis in ICI-treated. PAS-positive granules (large arrow) are more abundant in the basal region of a clear cell. There is an increase in the number of cytoplasmic vacuoles in the principal cells (small arrows). Sperm (Sp) appear normal in the cauda lumen on day 8. Bars = 25 μm for A, B. Bars = 12.5 μm for C, D.

epithelium was reduced in height as early as day 8. It is assumed that the decrease in epithelial height is related to the accumulation of luminal fluid; however, it may also be due to overgrowth of the rete epithelium because neonatal exposure to environmental estrogens has produced a similar dilation and overgrowth of the rete testis [29,30].

A prior study did not find these early effects of ICI 182,780 treatment [9]. However, here we report effects as early as day 4, at which time proximal regions of the efferent ductules were dilated. This observation is important because the dilatation did not induce a reduction in epithelial cell height, suggesting that the two effects are not directly linked. Others have suggested that the decrease in epithelial height is due to alterations in ion transporter

Table 2: Reproductive performance in mice after antiestrogen treatment[a].

Parameter	Control	ICI-Treated
Percent Progressive Sperm Motility	34.5 ± 2.90%	7.2 ± 3.11%[b,c]
Fertile males	6/6	2/6[d]
Average litter size	8.0 ± 0.8	5.80 ± 1.3[e]
Percentage of Resorptions/fetal deaths	12.3 ± 1.1%	20.67 ± 1.7%[c]

[a] N = 6 per group; mice were 118 days of age for fertility trials; 155 days of age at sacrifice. [b] Values are mean ± SEM [c] $p < 0.05$ by the chi-square test. [d] 4 of 6 males were infertile; subfertility was indicated by an increase in resorption in the 2 males that were fertile. [e] Not significantly different; $p = 0.21$ by t-test.

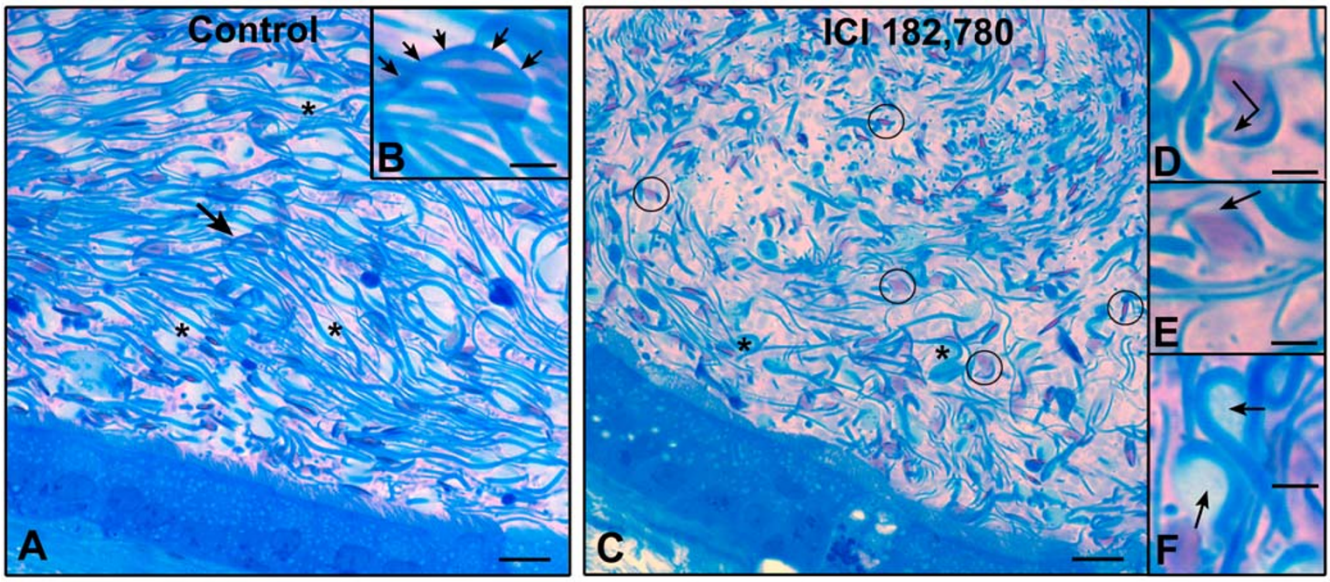

Figure 15
Cauda epididymal region on day 59 stained with Coomassie blue G250 to highlight the sperm acrosome and nucleus. A. Control section showing normal spermatozoa (arrow) with intact sperm tails and normal heads. Cytoplasmic droplets (*) are found along the mid-tail region. Sperm are aligned nearly parallel within the lumen. B. Higher magnification of a normal sperm from the control section showing an intact acrosome (arrows) along the dorsal edge of the sperm nucleus (pink stain). C. ICI-treated section showing more dilute sperm, isolated sperm heads (circles), disorganized appearance and sperm tails looped around the cytoplasmic droplets (*). D, E. higher magnification of ICI-treated sperm heads showing abnormal shapes (arrow) and decreased staining of the acrosome region. F. Higher magnification of the tail looped around cytoplasmic droplets (arrows). Bars = 10 μm for A, C. Bars = 2.5 μm for B, D, E, F.

expression [8], but the present study does not support this hypothesis, as fluid reabsorption detected by luminal dilation occurred without a decrease in epithelial height. Other early effects were subsequent reduction in efferent ductule epithelial height (day 8) and protrusion of the narrow cells in the epididymis. Effects on the testis were not observed until much later. These early morphological effects were maintained throughout the 125-day treatment period and are in agreement with our previous studies of αERKO mouse [4,5] and ICI 182,780 treatment in mice [9]. Thus, it may be possible to use the mouse antiestrogen treatment model during shorter periods of treatment for the study of fluid dynamics within the efferent ductules, but also to study testicular effects that require more than 50 days of exposure.

Overall effects of ICI 182,780 on the mouse efferent ductules were identical to those observed in the αERKO male, including the loss of NHE3 staining and decrease in staining for AQP-1 and CAII [7]. These data further support the hypothesis that estrogen's regulation of sodium transport by this epithelium is essential for maintenance

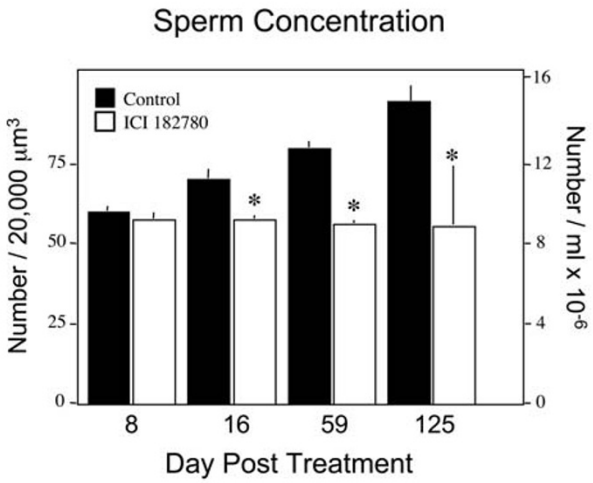

Figure 16
Sperm concentration from cauda epididymis in control and ICI-treated mice. The left Y-axis applies to days 8–59, which were analyzed by the optical dissector method. The right Y-axis applies to day 125, which were counted using the Hamilton Thorne semen analyzer system (Beverly MA). The data are presented as means ± SEM. Significant differences (*) between control and ICI-treated means are noted ($p < 0.05$).

of fluid reabsorption. Antiestrogen treatment also caused a decrease in ERα staining, which has been reported in female tissues [31], but the compound had no effect on ERβ.

The effects noted in epididymis could be due to direct action of ICI on the epididymal epithelium, as recent studies have shown that ERα is expressed more extensively in the epididymis of the mouse [21], than in the rat [11]. Cell types that responded to treatment, the narrow and apical cells of initial segment, apical cells of the caput, and clear cells of the corpus and cauda, are all strongly ERα-positive [21]. In the ICI treated group, apical vesicles in the narrow cells and vesicles in clear and principal cells in corpus and distal caudal epididymis were increased in size and number. An accumulation of large PAS-positive granules was also observed in the apical cells of the caput. These findings are nearly identical to epididymal changes seen in αERKO [5] and may indicate an attempt to increase reabsorption of fluid by the epididymis, to compensate for reduced reabsorption found in the proximal region of the efferent ductules [4,7].

In the control animals, epididymal sperm concentrations reached their peak on day 59, showing a gradual increase starting at 38 days of age. However, the ICI treated group did not experience this normal increase in sperm concentration and beginning on day 16 showed a divergence from controls so that on days 59 and 125 post treatment there were decreases of 30 and 41%, respectively. These differences are considerably more than the 22% decline seen in αERKO males [9]. On day 25 (data not shown), there was a 12.4% decline in sperm concentration, which was similar to our previous experiment, which showed an 11% decrease after 35 days of antiestrogen treatment [9]. Thus, the overall trend in the mouse antiestrogen treatment model is for increasing dilution of cauda sperm and accumulation of fluids in the efferent ductules and testis. It is noteworthy that the decrease in fertility did not occur until day 125 post treatment, the time period that coincided with the maximum decrease in sperm concentration. In the rat, decreased fertility coincided with the onset of testicular atrophy [14,15], therefore it was questioned whether infertility and subfertility was due to abnormal sperm maturation due to dilution in the epididymis or if atrophy of the seminiferous epithelium was required before sperm concentrations could reach levels that would produce infertility. The current study suggests that subfertility in the mouse antiestrogen treatment model is related to the sperm dilution effects that occur in the epididymis, which appears to induce abnormal maturation of the cauda sperm. Even in the αERKO male, testicular sperm are fertile when transplanted into germ cell depleted normal testes [12,13], which suggests that the epididymal environment is one of the more important factors leading to infertility in the absence of ERα expression in the male.

Conclusions

The antiestrogen, ICI 182,780 induces very early effects on rete testis, efferent ductules and epididymis, which resemble morphological changes observed in the αERKO male. These early effects are maintained throughout the treatment period of 125 days and thus, suggest that a much shorter model of 4–8 days of treatment may be used to study the role of estrogen in fluid reabsorption in the male tract. Although the inhibition of estrogen receptors for 125 days induced structural and physiological changes in the reproductive tract, it did not induce total testicular atrophy, but did cause a decrease in fertility and showed evidence of early induction of abnormal spermatogenesis. Thus, it is possible to induce infertility by blocking ER function in the male, without causing azoospermia. If such treatment effects are observed at lower dosages and if the responses are reversible, it should be possible in the future to target ERα for male contraception.

Authors' contributions

HWC carried out experiment one, analyzed the data and wrote the first draft of the manuscript. RN assisted with the immunohistochemistry. KC provided general labora-

tory assistance, carried out experiments 2–3 and assisted with photography. NAQS provided valuable laboratory assistance. RAH served as PI on this project, designed the study and wrote the final draft. All authors read and approved the final manuscript.

Acknowledgements

We are grateful for the generous supply of ICI 182,780 provided by AstraZeneca, Macclesfield, UK. Supported by NIH grant number HD35126 (RAH) and partially supported by the Foundation of Sunchon National University (H.W.C) and CONRAD.

References

1. Eddy EM, Washburn TF, Bunch DO, Goulding EH, Gladen BC, Lubahn DB and Korach KS: **Targeted disruption of the estrogen receptor gene in male mice causes alteration of spermatogenesis and infertility.** *Endocrinol* 1996, **137:**4796-4805.
2. Lubahn DB, Moyer JS, Golding TS, Couse JF, Korach KS and Smithies O: **Alteration of reproductive function but not prenatal sexual development after insertional disruption of the mouse estrogen receptor gene.** *Proc Natl Acad Sci USA* 1993, **90:**11162-11166.
3. Dupont S, Krust A, Gansmuller A, Dierich A, Chambon P and Mark M: **Effect of single and compound knockouts of estrogen receptors a (ER a) and b (ER b) on mouse reproductive phenotypes.** *Development* 2000, **127:**4277-4291.
4. Hess RA, Bunick D, Lee KH, Bahr J, Taylor JA, Korach KS and Lubahn DB: **A role for oestrogens in the male reproductive system.** *Nature* 1997, **390:**509-512.
5. Hess RA, Bunick D, Lubahn DB, Zhou Q and Bouma J: **Morphologic changes in efferent ductules and epididymis in estrogen receptor-alpha knockout mice.** *J Androl* 2000, **21:**107–121.
6. Nakai M, Bouma J, Nie R, Zhou Q, Carnes K, Jassim E, Lubahn DB and Hess RA: **Morphological analysis of endocytosis in efferent ductules of estrogen receptor-alpha knockout male mouse.** *Anat Rec* 2001, **263:**10-18.
7. Zhou Q, Clarke L, Nie R, Carnes K, Lai LW, Lien YH, Verkman A, Lubahn D, Fisher JS, Katzenellenbogen BS and Hess RA: **Estrogen action and male fertility: Roles of the sodium/hydrogen exchanger-3 and fluid reabsorption in reproductive tract function.** *Proc Natl Acad Sci U S A* 2001, **98:**14132-14137.
8. Lee KH, Finnigan-Bunick C, Bahr J and Bunick D: **Estrogen Regulation of Ion Transporter Messenger RNA Levels in Mouse Efferent Ductules Are Mediated Differentially Through Estrogen Receptor (ER) alpha and ERbeta.** *Biol Reprod* 2001, **65:**1534-1541.
9. Lee KH, Hess RA, Bahr JM, Lubahn DB, Taylor J and Bunick D: **Estrogen receptor alpha has a functional role in the mouse rete testis and efferent ductules.** *Biol Reprod* 2000, **63:**1873-1880.
10. Couse JF, Hewitt SC, Bunch DO, Sar M, Walker VR, Davis BJ and Korach KS: **Postnatal sex reversal of the ovaries in mice lacking estrogen receptors alpha and beta.** *Science* 1999, **286:**2328-2331.
11. Hess RA, Zhou Q and Nie R: **The Role of Estrogens in the Endocrine and Paracrine Regulation of the Efferent Ductules, Epididymis and Vas deferens.** *The Epididymis: from Molecules to Clinical Practice* Edited by: *Robaire B and Hinton B T. New York, Kluwer Academic/Plenum Publishers*; 2002:317-338.
12. Mahato D, Goulding EH, Korach KS and Eddy EM: **Estrogen receptor-alpha is required by the supporting somatic cells for spermatogenesis.** *Mol Cell Endocrinol* 2001, **178:**57-63.
13. Mahato D, Goulding EH, Korach KS and Eddy EM: **Spermatogenic cells do not require estrogen receptor-alpha for development or function [see comments].** *Endocrinology* 2000, **141:**1273-1276.
14. Oliveira CA, Carnes K, Franca LR and Hess RA: **Infertility and testicular atrophy in the antiestrogen-treated adult male rat.** *Biol Reprod* 2001, **65:**913-920.
15. Oliveira CA, Zhou Q, Carnes K, Nie R, Kuehl DE, Jackson GL, Franca LR, Nakai M and Hess RA: **ER Function in the Adult Male Rat: Short- and Long-Term Effects of the Antiestrogen ICI 182,780 on the Testis and Efferent Ductules, without Changes in Testosterone.** *Endocrinology* 2002, **143:**2399-2409.
16. Nie R, Zhou Q, Jassim E, Saunders PT and Hess RA: **Differential expression of estrogen receptors a and b in the reproductive tracts of adult male dogs and cats.** *Biol Reprod* 2002, **66:**1161-1168.
17. Saunders PT, Millar MR, Williams K, Macpherson S, Harkiss D, Anderson RA, Orr B, Groome NP, Scobie G and Fraser HM: **Differential expression of estrogen receptor-alpha and -beta and androgen receptor in the ovaries of marmosets and humans.** *Biol Reprod* 2000, **63:**1098-1105.
18. Prins GS: **Neonatal estrogen exposure induces lobe-specific alterations in adult rat prostate androgen receptor expression.** *Endocrinology* 1992, **130:**3703-3714.
19. Prins GS and Birch L: **The developmental pattern of androgen receptor expression in rat prostate lobes is altered after neonatal exposure to estrogen.** *Endocrinology* 1995, **136:**1303-1314.
20. Howell A, Osborne CK, Morris C and Wakeling AE: **ICI 182,780 (Faslodex): development of a novel, "pure" antiestrogen.** *Cancer* 2000, **89:**817-825.
21. Zhou Q, Nie R, Prins GS, Saunders PT, Katzenellenbogen BS and Hess RA: **Localization of androgen and estrogen receptors in adult male mouse reproductive tract.** *J Androl* 2002, **23:**870-881.
22. Saunders PT, Fisher JS, Sharpe RM and Millar MR: **Expression of oestrogen receptor beta (ER beta) occurs in multiple cell types, including some germ cells, in the rat testis.** *J Endocrinol* 1998, **156:**R13-7.
23. Saunders PTK, Maguire SM, Gaughan J and Millar MR: **Expression of oestrogen receptor beta (ER-beta) in multiple rat tissues visualised by immunohistochemistry.** *Journal of Endocrinology* 1997, **154:**R 13-R 16.
24. Goyal HO, Bartol FF, Wiley AA and Neff CW: **Immunolocalization of receptors for androgen and estrogen in male caprine reproductive tissues: unique distribution of estrogen receptors in efferent ductule epithelium.** *Biol Reprod* 1997, **56:**90-101.
25. Fisher JS, Millar MR, Majdic G, Saunders PT, Fraser HM and Sharpe RM: **Immunolocalisation of oestrogen receptor-alpha within the testis and excurrent ducts of the rat and marmoset monkey from perinatal life to adulthood.** *J Endocrinol* 1997, **153:**485-495.
26. Vaillant S, Magre S, Dorizzi M, Pieau C and Richard-Mercier N: **Expression of AMH, SF1, and SOX9 in gonads of genetic female chickens during sex reversal induced by an aromatase inhibitor.** *Dev Dyn* 2001, **222:**228-237.
27. Robertson KM, O'Donnell L, Simpson ER and Jones ME: **The phenotype of the aromatase knockout mouse reveals dietary phytoestrogens impact significantly on testis function.** *Endocrinology* 2002, **143:**2913-2921.
28. Krege JH, Hodgin JB, Couse JF, Enmark E, Warner M, Mahler JF, Sar M, Korach KS, Gustafsson JA and Smithies O: **Generation and reproductive phenotypes of mice lacking estrogen receptor beta.** *Proc Natl Acad Sci USA* 1998, **95:**15677-15682.
29. Aceitero J, Llanero M, Parrado R, Pena E and Lopez-Beltran A: **Neonatal exposure of male rats to estradiol benzoate causes rete testis dilation and backflow impairment of spermatogenesis.** *Anat Rec* 1998, **252:**17-33.
30. Fisher JS, Turner KJ, Brown D and Sharpe RM: **Effect of neonatal exposure to estrogenic compounds on development of the excurrent ducts of the rat testis through puberty to adulthood.** *Environ Health Perspect* 1999, **107:**397-405.
31. Howell A: **Faslodex (ICI 182780). an oestrogen receptor downregulator.** *Eur J Cancer* 2000, **36:**S87-8.